Analyzing the Progressive Damage of Composites Due to Manufacturing Induced Defects Through a Semi-Discrete Damage Model

SAI KRISHNA MEKA, RYAN ENOS and DIANYUN ZHANG

ABSTRACT

During composite manufacturing processes, multiple steps are involved, each step introducing new physical and chemical processes. These processes alter the properties of the constituents (fiber and matrix), affecting the behavior of the composite materials. The changes in the properties of the fiber are not that significant. Whereas the mechanical and thermal properties of the matrix such as Young's modulus, Poisson's ratio, coefficient of thermal expansion etc. change significantly. Residual stresses are developed in the composite due to thermal expansion mismatch of the constituents and cure shrinkage of the resin. These resulting residual stresses have a considerable impact on the mechanical properties and performance of the composites. Also, cracks develop in the composite system during the manufacturing process which can affect the performance of the composite.

When the composite system with residual stresses is mechanically loaded, the system exhibits a drop in the strength after a critical stress state is reached. To predict the critical stress at which the drop occurs we use the continuum damage method called the Smeared Crack Approach (SCA). Using SCA we can predict the stress-strain behavior of an RVE as the damage progresses. The critical stress value of the microscale RVE acts as the corresponding strength of the composite on a macro-scale level.

To account for the variability in a composite system we randomly generate different RVEs. This is done by varying the number of fibers and the location of fibers using a statistic distribution for a fixed volume fraction. Then we conduct the simulations of manufacturing and progressive damage to identify the strength values of the RVEs.

The strength values obtained are then used to assign to the different regions of a semi-discrete damage model of a composite laminate in macro-scale. The unique aligned meshing strategy of the model decomposes the bulk non-linearity and localization zones which provide a proper load transfer pathway. This random assignment of the strength values simulates the realistic behavior of a composite where each region has almost the same material properties but different strength values due to the uncertainties associated with the manufacturing processes.

Sai Krishna Meka, Graduate Research Assistant, Purdue University, West Lafayette, IN 47907 Ryan Enos, Graduate Research Assistant, Purdue University, West Lafayette, IN 47907 Dianyun Zhang, Associate Professor, Purdue University, West Lafayette, IN 47907

INTRODUCTION

Fiber-reinforced composites are used extensively in the transportation sector to prepare light weight structural components. The manufacturing of these composites takes place at high temperatures to ensure the complete curing of the resin. However, the manufacturing process induces defects in the matrix because of which there is a significant difference between the neat resin matrix properties and the in-situ matrix properties. These manufacturing-induced effects have been investigated in the existing literature, but there was no quantitative relationship developed to determine how these manufacturing effects are influencing the deviation of the in-situ matrix properties from that of the neat resin properties.

The present work aims to address this issue by incorporating the manufacturing induced effects to predict the composite laminate's non-linear behavior when mechanically loaded. This is done by incorporating the effects of the fiber distribution and accounting for the residual stresses that develop in a representative volume element (RVE). We run simulation of the manufacturing process on the RVE which leads to development of residual stresses. This information of residual stresses is used when the RVEs are simulated with a mechanical loading.

When the RVE is mechanically loaded, initially the stress-strain relationship is linear because of the linear elasticity. However, when a critical stress state is reached i.e., the when the micro-cracks in the matrix coalesce into macro cracks the stress starts decreasing with the increase in strain. This progressive damage analysis is performed by using the continuum smeared crack method in this paper called the Smeared Crack Approach. The advantage of using continuum damage models over the discrete damage models is that the computational costs and modeling effort is significantly lower. However, in the case of continuum smeared crack methods, the fidelity may be lower than that of a discrete crack model. Fidelity is the ability of a model to capture stress gradients, such as those that occur near notches, free edges and cracks, and the ability to resolve details such as the type of cracks, interactions between cracks etc. It is found in literature that in order to capture the directionality of a matrix crack with a comparable mesh size, a passive control of the crack directionality can be introduced by using fiber aligned meshes. The current model aims for high discreteness for capturing sharp matrix cracks, while retaining the benefits of the efficiency of smeared crack approaches. This method is therefore characterized as a semi-discrete damage model [1].

The critical stress values of the composite that are obtained from the microscale RVE model are used as the strength values for the macroscale model in the fiber aligned semi discrete damage approach. The dominant mode of in-plane failure is the matrix failure, the cohesive modeling between plies also must be accounted for apart from modeling each ply individually.

CONSTITUTIVE MODEL

To model the progressive damage of composites, the two widely used models are the continuum smeared crack methods (CSCM) and discrete crack methods (DCM). But the computational costs of discrete methods rise as the number of components to be modeled increases. Therefore, it is impractical to model the response of a large structure with multiple failure mechanisms present in a geometrically nonlinear setting. CSCM

are often more efficient compared to DCM, however, the fidelity may be lower. Compared to the explicit modelling of cracks, in the CSCM, the effect of cracks is modeled during progressive failure much more efficiently. To construct the constitutive law for the post-peak behavior of the composite, we adopted the Smeared Crack Approach (SCA). In the SCA, the effect of the micro-cracks is smeared over a characteristic length. This smearing effect is mathematically characterized by deteriorating the secant stiffness of the material as the damage progresses once the transition criteria is satisfied.

The transition criteria (failure criteria) used for each of the plies is the maximum stress criteria. When the local stresses reach the critical strength value, we conclude that failure has initiated and the material transitions from pre-peak behavior to post-peak behavior. The pre-peak behavior corresponds to the matrix micro damage due to the growth of voids and flaws in the matrix, while the post-peak behavior corresponds to the accumulation of matrix micro damage which leads to matrix macroscopic cracking. The pre-peak behavior is governed by a linear elastic constitutive law, i.e., a strain-based formulation, while in the post-peak regime the softening of the material is captured by a displacement-based formulation of linear traction separation law [4].

In the pre-peak regime, standard continuum descriptions of the material are assumed to hold. In the post-peak regime, it is assumed that the total strain (ε) may be split up into a continuum part and a crack part.

$$\varepsilon = \varepsilon^{co}$$
 (in the pre-peak regime) (1)

$$\varepsilon = \varepsilon^{co} + \varepsilon^{cr}$$
 (in the post-peak regime) (2)

The continuum strain (ε^{co}) can further be decomposed as a sum of the elastic (ε^{el}) , plastic (ε^{pl}) and thermal strain (ε^{th}) contributions as shown below:

$$\varepsilon^{co} = \varepsilon^{el} + \varepsilon^{pl} + \varepsilon^{th} \tag{3}$$

In the current formulation, we are not considering any plasticity to be present. Therefore $\varepsilon^{co} = \varepsilon^{el} + \varepsilon^{th}$. The relation between the local crack strains and the global crack strains as shown in equation (4) below:

$$\varepsilon^{cr} = N e^{cr} = N \begin{bmatrix} \varepsilon_{nn}^{cr} \\ \gamma_{t1}^{cr} \\ \gamma_{t2}^{cr} \end{bmatrix}$$
(4)

Similarly, global stress (σ) can be transformed to yield the tractions at the crack interface (s^{cr}):

$$s^{cr} = \begin{bmatrix} \sigma_{nn}^{cr} \\ \tau_{t1}^{cr} \\ \tau_{t2}^{cr} \end{bmatrix} = N^T \sigma \tag{5}$$

The tractions at the crack interface are related to the crack strain through the secant stiffness matrix and a damping matrix by

$$s^{cr} = D^{cr}e^{cr} + D^{da}e^{\dot{c}r} \tag{6}$$

The damping matrix makes the crack progression a time-dependent property. It is used to smoothen the numerical solution scheme. Any numerical scheme involves a discrete time step. The crack strain rate is accordingly approximated with finite differences

The relation between the total stiffness (global) i.e. " σ " and the total strain (global) i.e. " ε " is:

$$\sigma = D^{co}\varepsilon \tag{7}$$

Where (D^{co}) is the continuum stiffness matrix, given by $S^{co^{-1}}$ and (S^{co}) is compliance matrix given as follows for an isotropic material:

$$S^{co} = \begin{bmatrix} 1/E & -\nu/E & -\nu/E & 0 & 0 & 0 \\ -\nu/E & 1/E & -\nu/E & 0 & 0 & 0 \\ -\nu/E & -\nu/E & 1/E & 0 & 0 & 0 \\ 0 & 0 & 0 & 2(1+\nu)/E & 0 & 0 \\ 0 & 0 & 0 & 0 & 2(1+\nu)/E & 0 \\ 0 & 0 & 0 & 0 & 0 & 2(1+\nu)/E \end{bmatrix}$$
(8)

 (S^{co}) for a transversely isotropic material is given as shown in equation (9).

$$S^{co} = \begin{bmatrix} 1/E_1 & -\nu_{12}/E_1 & -\nu_{12}/E_1 & 0 & 0 & 0\\ -\nu_{12}/E_1 & 1/E_2 & -\nu_{23}/E_2 & 0 & 0 & 0\\ -\nu_{12}/E_1 & -\nu_{23}/E_2 & 1/E_2 & 0 & 0 & 0\\ 0 & 0 & 0 & 1/G_{12} & 0 & 0\\ 0 & 0 & 0 & 0 & 1/G_{12} & 0\\ 0 & 0 & 0 & 0 & 0 & 2(1+\nu_{23})/E_2 \end{bmatrix}$$
(9)

Combining all equations results in an implicit relation between the crack strain and the total elastic strain.

$$e^{cr} = \left[D^{cr}(e^{cr}) + N^T D^{co} N + \frac{1}{\Delta t} D^{da} \right]^{-1} \left[N^T D^{co} \varepsilon^{cr} + \frac{1}{\Delta t} D^{da} e^{cr}_{old} \right]$$
(10)

Finally, the relation between total stress and total strain in the post-peak regime is formulated as

$$\sigma = \left[D^{co} - D^{co} N \left(D^{cr} + N^T D^{co} N + \frac{1}{\Delta t} D^{da} \right)^{-1} N^T D^{co} \right] \varepsilon^{cr} - \frac{1}{\Delta t} \left[D^{cr} (e^{cr}) + N^T D^{co} N + \frac{1}{\Delta t} D^{da} \right]^{-1} D^{da} e^{cr}_{old}.$$
 (11)

The *total* stress-strain description, such as equation (11), which is more suited for large time increments during reversed loading, is pursued here. Equation (10) is a highly non-linear equation for the crack strain. It is solved via Newton's method by defining a function that is to be minimized. Along with this, it is also required to account for the mismatch of the thermo-mechanical properties of the constituent fiber and matrix which lead to the build-up of the residual stresses inside the composite which will influence the failure response of the composite under the subsequent loading.

SCA for the Matrix

When we are formulating the relations for the smeared crack formulation for a matrix the continuum stiffness matrix (D^{co}) and the compliance matrix (S^{co}) should be for an isotropic material as shown in equation 8.

SCA for the Composite

But, when formulating the relations for smeared crack approach in the composite, the continuum stiffness matrix (D^{co}) and the compliance matrix (S^{co}) should be for a transversely isotropic material as shown in equation 9.

This is important to understand that we first use SCA for the matrix when working on the microscale level of a composite. We assume that the crack can only form and propagate in the matrix whereas the fiber is assumed to not undergo any cracking and damage. In the macroscale when we are modeling the laminate by homogenizing the composite properties, there we use SCA for the composite which will be further explained in the following sections of the paper.

RVE GENERATION

In order to understand the residual stresses developed in a composite system during the manufacturing process and the impact it has on the progressive damage of the composite it is sufficient to just look at the 'cooling' (temperature drop) part of the curing cycle from the vitrification point to the end of the curing cycle [3]. The simulation of the cooling (temperature drop) is conducted on a randomly generated RVE by specifying the fiber volume fraction and the number of fibers we want to be present within this RVE. The idea behind conducting simulations on a randomly generated RVE is to be able to capture the randomness and uncertainty that is associated with the manufacturing process where it is not necessary that all the fibers are equidistant from each other and are packed in ideal configurations such as square packing or hexagonal packing.

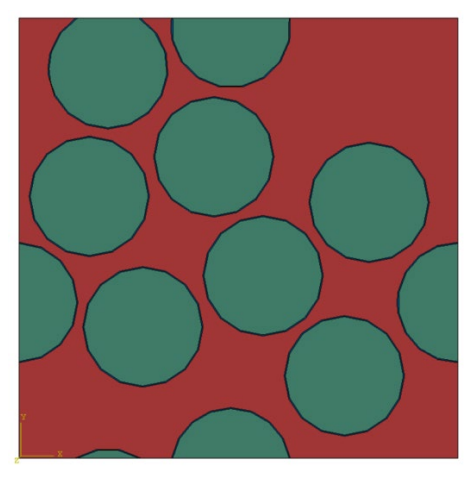


Figure 1. Randomly generated RVE.

Figure 1 shows a randomly generated RVE which has 9 fibers in it and has a fiber volume fraction of around 51%. Upon conducting a simulation of the temperature drop from 383.15 K (glass transition temperature of resin) to the room temperature 298.15 K the residual stress profile that is developed in the RVE is as shown in figure 2. Further when the RVE is mechanically loaded the progressive damage simulation is done by applying the concept of Smeared Crack Approach (SCA) the stress vs strain plot is obtained as shown in figure 3 and the crack contour plot is as shown in the figure 4. The red elements in figure 4 are the ones that have failed; hence the red elements together are how the crack path looks like.

The curing cycle parameters of the matrix (EPON 862/W) are as listed in table I. The matri and fiber (Carbon) properties of the composite system are as listed in table II and table III respectively.

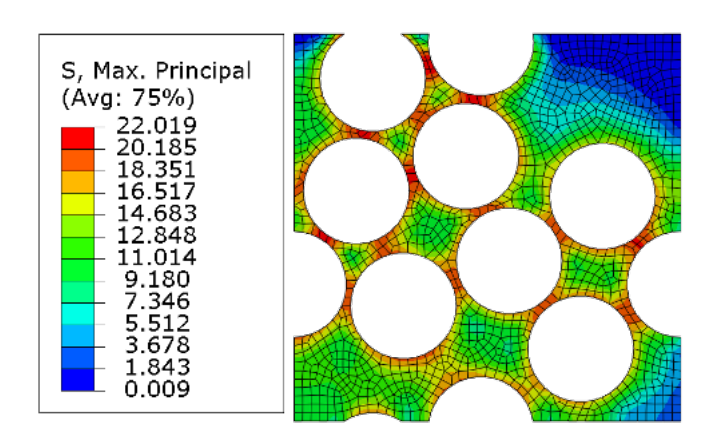


Figure 2. Residual stress contour in RVE that undergoes cure cycle (cooling) simulation.

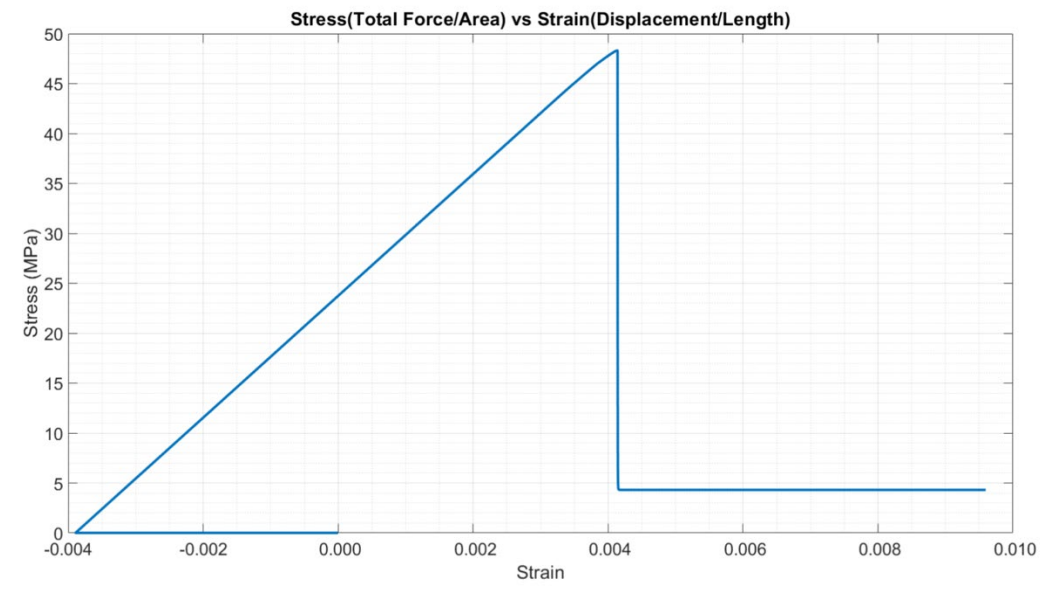


Figure 3. Stress vs Strain plot for RVE with residual stress that undergoes mechanical loading.

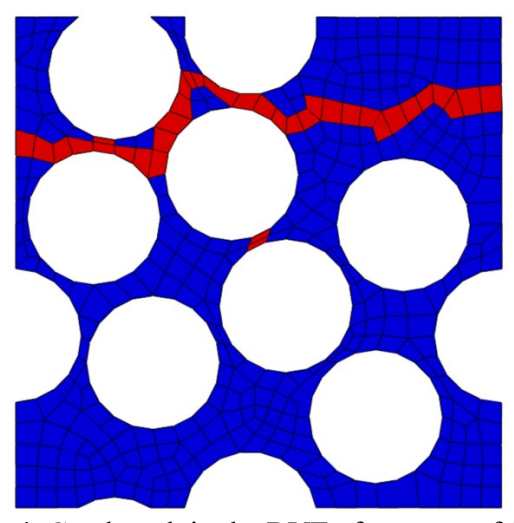


Figure 4. Crack path in the RVE after onset of failure

TABLE I. THERMO-CHEMO-MECHANICAL PROPERTIES OF THE EPON 862/W SYSTEM.

Symbol	Definition	Value	Unit
$ ho_m$	Density	1200	kg/m ³
$C_{p,m}$	Specific Heat	1150	J/kg/K
k_m	Thermal	0.188	W/m/K
	Conductivity		
α_m^R	CTE at the rubbery	1.82E-04	1/K
	state		

$lpha_m^G$	CTE at the glassy	7.78E-05	1/K
	state		
v_{sh}^{T}	Chemical	-0.0372	-
	shrinkage		
	(volume)		
E_m^R	Modulus at the	32.4E+06	Pa
	rubbery state		
E_m^G	Modulus at the	3.24E+09	Pa
	glassy state		
v_m^G	Poisson's ratio at	0.35	
	the glassy state		
T_q^0	Glass transition	246	K
9	temperature of		
	fully cured resin		
T_g^{∞}	Glass transition	383	K
9	temperature of		
	uncured resin		
λ	Fitting parameter	0.39	
ϕ_{gel}	DOC at gelation	0.71	-

TABLE II. MATRIX MATERIAL PROPERTIES.

Quantity	Description	Value
E_m	Young's Modulus	3240 MPa
$ u_m$	Poisson's Ratio	0.35
σ_{cr}^0	Critical Stress	70 MPa
G_{IC}	Fracture Energy (Mode-1)	0.32 kJ/m^2

TABLE III. CARBON FIBER PROPERTIES.

Quantity	Description	Value
E_1	Young's Modulus	231 GPa
	(Longitudinal)	
$E_2 = E_3$	Young's Modulus	15 GPa
	(Transverse)	
$v_{12} = v_{13}$	Poisson's ratio 12 and 13	0.27
v_{23}	Poisson's ratio 23	0.497
$G_{12} = G_{13}$	Shear Modulus in 12 and	24 GPa
_	13	
G_{23}	Shear Modulus in 23	5.01 GPa
α_1	Coefficient of thermal	-9E-07 K ⁻¹
_	expansion (longitudinal)	
$\alpha_2 = \alpha_3$	Coefficient of thermal	7.2E-06 K ⁻¹
	expansion (transverse)	

STRENGTH DISTRIBUTION

As discussed earlier there is lot of stochasticity in the process of RVE generation as the fiber placement can be varied randomly. Ideally, we should be conducting several experiments on the composite and look at the micrographs of the composite to understand the fiber placement and the fiber density in the matrix and observe the peak stress attained. Then conduct statistical inference on the peak stress data that we have and estimate an appropriate statistical distribution of the peak stresses which now act as the values for strength in the composite. This distribution should be used to assign the strength values in the fiber aligned thin strips in our semi discrete damage model.

However, conducting several such experiments is tedious to infer a distribution and it is just as good as assuming a distribution for the strength values from an engineering standpoint. Therefore, we assume a uniform strength distribution for the longitudinal and transverse strengths of the composite and assign strength values to the fiber aligned thin strips. We are assuming the maximum and minimum strength values for both transverse and longitudinal strengths as specified in table IV for the IM7/8552 system.

TABLE IV. IM7/8522 SYSTEM PROPERTIES.

Property	Description	Value
E ₁	Young's Modulus (Longitudinal)	128 GPa
$E_2 = E_3$	Young's Modulus (Transverse)	7.6 GPa
$G_{12}=G_{13}$	In-plane Shear Modulus	4.4 GPa
G_{23}	Out of plane Shear Modulus	2.62 GPa
$\nu_{12} = \nu_{13}$	In-plane Poisson's Ratio	0.35
ν_{23}	Out of plane Poisson's Ratio	0.45
$X_T(\max), X_T(\min)$	Longitudinal Strength (in Tension)	2415MPa, 2300 MPa
$X_C(max), X_C(min)$	Longitudinal Strength (in Compression)	1607.55 MPa, 1531 MPa
$Y_T(max), Y_T(min)$	Transverse Strength (in Tension)	96.8 MPa, 44 MPa
Y_C	Transverse Strength (in Compression)	250 MPa
$S_{12}(max), S_{12}(min)$	In-plane Shear Strength	112.11MPa, 78.4 MPa
S_{23}	Out of plane Shear Strength	78 MPa
G_{1C}^F	Fracture energy of the fiber (longitudinal)	40 kJ/m^2

G_{2C}^F	Fracture energy of	4 kJ/m^2
	the fiber (transverse)	
G_{IC}^{M}	Fracture energy of	2 kJ/m^2
	the matrix	
	(longitudinal)	
G_{2c}^{M}	Fracture energy of	1 kJ/m^2
	the matrix	
	(transverse)	

SEMI-DISCRETE FINITE ELEMENT MODEL

To analyze the progressive failure analysis of the composite laminate in uniaxial tension, a novel semi-discrete damage model is used as discussed in [2]. In the semi-discrete damage model fiber-aligned meshes are employed in order to increase the fidelity of the model as opposed to model without aligned meshing strategy. Along with using a semi-discrete finite element model, it is also necessary to make a smart choice when it comes to meshing the model by balancing both efficiency and fidelity [3].

The semi-discrete finite element model is developed by decomposing the model into two regions, a bulk material region and a discrete region consisting of thin strips of elements. This idea is adopted from [1]. All regions are modeled with pre-peak linearity, that is, the constitutive law for a linear elastic material, but the failure modes are separated into these two distinct regions. Matrix splitting failure is only active in the thin strips, while fiber failure is active in every element. The efficiency is maintained by using only continuum elements. To capture the intra-ply damage, semi-discrete crack method (SDCM) is used, while for the inter-ply damage surface-based cohesive contact interaction is employed.

Fiber-aligned meshes are created after we have made partitions to create the thin strips in which matrix splitting failure mode is active. Once these thin strips are created, we assign mesh controls such that the bulk regions are assigned free mesh control, while the matrix-cracking strips are meshed with structured HEX elements. The reason behind this is to ensure that a strip is modeled with exactly one element along the transverse direction. Randomization is brought into the model by now assigning the values of strength based on the strength distributions that we have to these thing strip sections in the model. This is achieved by writing a python code as a part of the script to generate the ABAQUS model.

The partition procedure can be tedious to do in ABAQUS GUI, therefore, we resort to python scripting as this enables us to have the flexibility of choosing the spacing between the thin strips and choosing the thickness of the strips. The appropriate thickness of the strips is achieved by following the convention shown in equation 12 as mentioned in [2].

$$d_{cr} = \min\left\{\frac{s}{10}, \frac{t_{ply}}{2}\right\} \tag{12}$$

Where d_{cr} is the thickness of the strips, s is the spacing between the thin strips, and t_{ply} is the thickness of each ply. The dimensions used for the laminate model are as shown in the figure (5) and figure (6). The cohesive zone thickness is 9.525×10^{-3} mm,

the ply thickness value is 190.50×10^{-3} mm. The total laminate thickness is therefore 790.575×10^{-3} mm. The length of the laminate is 114.3 mm, and the width of laminate is 0.8 mm. We need to have an elastic boundary at the end of the laminate specimen so that failure doesn't occur at the boundaries when the specimen is loaded in tension. There must be a transition region from the boundary to the laminate as shown in the figure () so that there is smoothening of the mesh between the elastic boundary and the gage section of the laminate. The width of mesh transition region was chosen to be half the width of the elastic boundary. Width of elastic boundary being 5.175 mm.



Figure 5. Thickness dimensions in the [+45/-45/-45/+45] laminate.

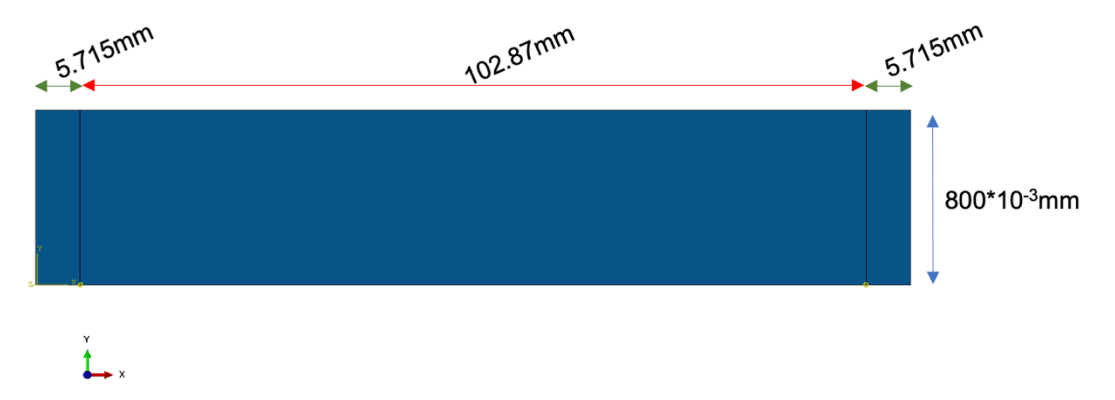


FIGURE 6. Length and width dimensions of the [+45/-45/-45/+45] laminate.

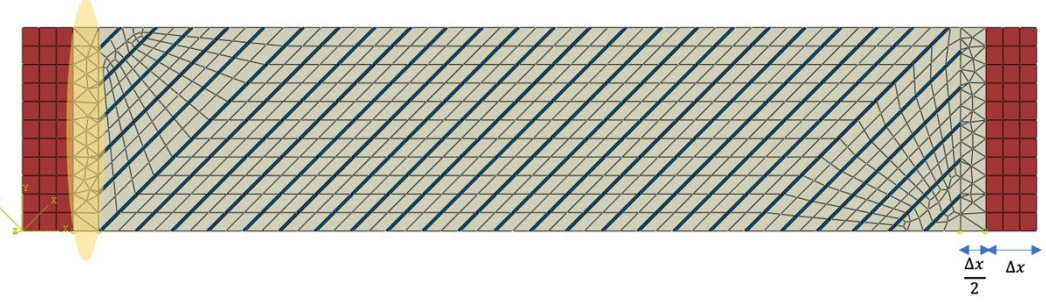


FIGURE 7. Depicting mesh transition region in +45 ply with aligned mesh.

RESULTS AND DISCUSSION

We perform the tensile loading simulation on the unnotched composite laminate model with aligned mesh and enabling randomization of the strength properties. The effect of randomization is observed in the figure 8. The peak stress obtained in both the cases is 131.95 MPa and the Young's modulus value of pre-peak regime is 15081.71 MPa. The closed form solution however shows that the peak stress is 156.80 MPa and the Young's modulus value of pre-peak regime is 15658.57 MPa. The mismatch in the peak stress value of the simulation and the closed form solution is significant. It makes sense that the peak stress value is lesser than that of the closed form solution. The reason for this might be that the onset of failure can happen at multiple places in the laminate instead of happening at just one place. Due to the onset of failure at multiple places, the laminate would fail at a lower stress value than the closed form value. Similarly, the young's modulus of the simulation model would be lesser than the closed value for the same reason. It is interesting to observe that the pre-peak stress-strain performance of the laminate without randomization also happens to have similar behavior as the laminate in which randomization is enabled.

While the simulation results carry meaning and the whole procedure outlines a framework on how the effects of manufacturing can be incorporated in the progressive damage of a composite laminate, it is important to corroborate these results with experimental data.

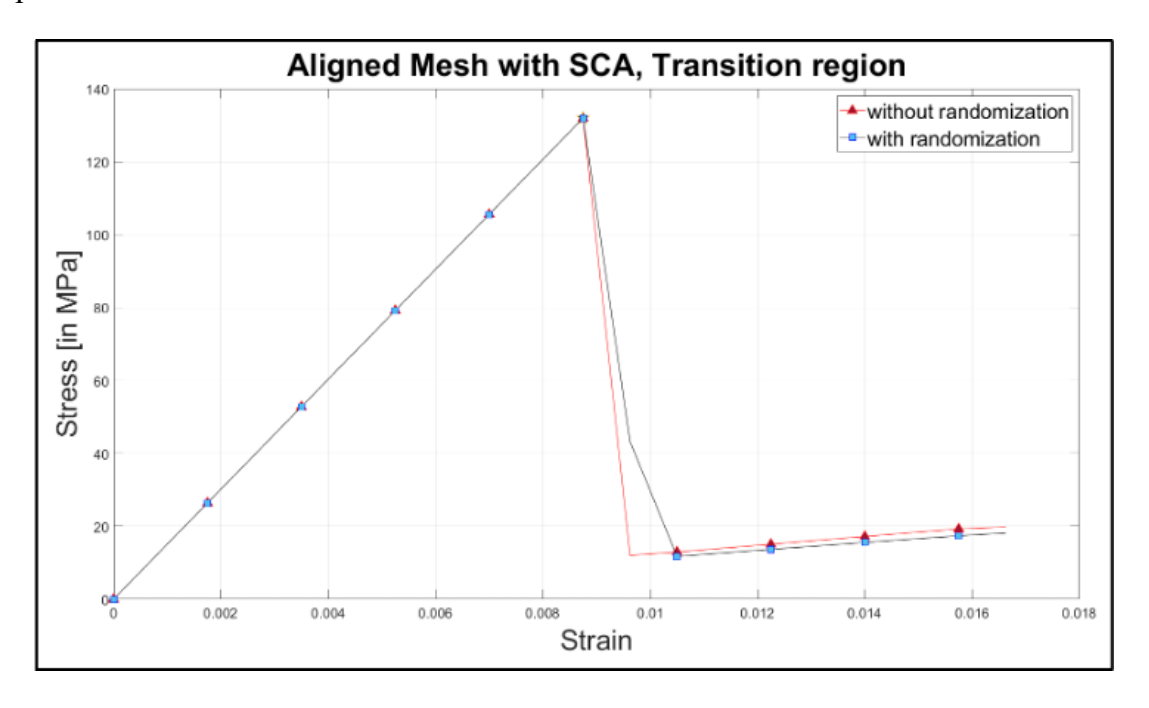


FIGURE 8. Stress vs Strain plot of the laminate with and without randomization.

REFERENCES

1. M. H. Nguyen, A. M. Waas, A novel mode-dependent and probabilistic semi-discrete damage model for progressive failure analysis of composite laminates - part i: Meshing strategy and mixed-mode law, Composites Part C: Open Access 3 (2020) 100073.

- 2. M. H. Nguyen, A. M. Waas, A novel mode-dependent and probabilistic semi-discrete damage model for progressive failure analysis of composite laminates part ii: Applications to unnotched and openhole tensile specimens, Composites Part C: Open Access 3 (2020) 100071.
- 3. S. K. Meka, R. Enos, D. Zhang, Effects of manufacturing processes on progressive damage of composites, in: Proceedings of the ASME Aerospace Structures, Structural Dynamics, and Materials Conference (SSDM)
- 4. Z. Bazant, B. Oh, Crack band theory for fracture of concrete, Mat eriaux et Constructions 16142 (1983) 155–177.